

# Electronic Supplementary Materials 2 – Description of the musculoskeletal model

This document is an electronic supplementary material (ESM2) for the article entitled “*Influence of force-length relationship and task-specific constraints on finger force-generating capacities*”

## Article information

### **INFLUENCE OF FORCE-LENGTH RELATIONSHIP AND TASK-SPECIFIC CONSTRAINTS ON FINGER FORCE-GENERATING CAPACITIES**

Goislard de Monsabert B<sup>1</sup>, Caumes M<sup>1</sup>, Berton E<sup>1</sup>, Vigouroux L<sup>1</sup>.

<sup>1</sup>Aix Marseille Univ, CNRS, ISM, Marseille, France

Correspondence: Benjamin GOISLARD DE MONSABERT

[benjamin.goislard-de-monsabert@univ-amu.fr](mailto:benjamin.goislard-de-monsabert@univ-amu.fr)

## Global description of the model

The same musculoskeletal model as the study focusing on power grip<sup>2</sup> was used to estimate the force ( $F^m$ ) and length ( $L^m$ ) of *flexor digitorum superficialis* (FDS), *extensor digitorum communis* (EDC), *flexor carpi radialis* (FCR) and *extensor carpi radialis* (ECR). The principle of the model is described in. The model is divided in three steps (Figure ESM3iA): muscle-tendon unit kinematics, muscle belly excursion, and force-length-activation relationships. The equations and data corresponding to muscle belly excursion and force-length-activation were determined in previous studies<sup>6,7</sup> from motion capture, ergometer, ultrasound imaging and electromyography data during maximal isometric contractions.

## Muscle-tendon unit kinematics

The current muscle-tendon unit (MTU) length ( $L^{mtu}$ ) was determined from the measured reference MTU length ( $L_r^{mtu}$ ) and joint angles ( $\theta^j$ ) using geometrical models representing the path of the tendon around each joint as a function of its current angular position. The current MTU length was calculated by adding to  $L_r^{mtu}$  the total MTU excursion corresponding to the sum of excursion at each individual joint ( $\Delta L_j^{mtu}$ ).

$$L^{mtu} = L_r^{mtu} + \sum_j \Delta L_j^{mtu} \quad \text{Equation 1}$$

With  $j$  corresponding to one of the four joints, i.e., wrist (WR), distal (DIPi) or proximal (PIPi) interphalangeal or metacarpophalangeal (MCPI) joint. The excursion was null when tendon

was not crossing the joint such that  $\Delta L_{DIPi}^{MTU} = 0$  for FDS and  $\Delta L_{DIPi}^{MTU} = \Delta L_{PIPi}^{MTU} = \Delta L_{MCPi}^{MTU} = 0$ . wrist prime movers (ECR, FCR).

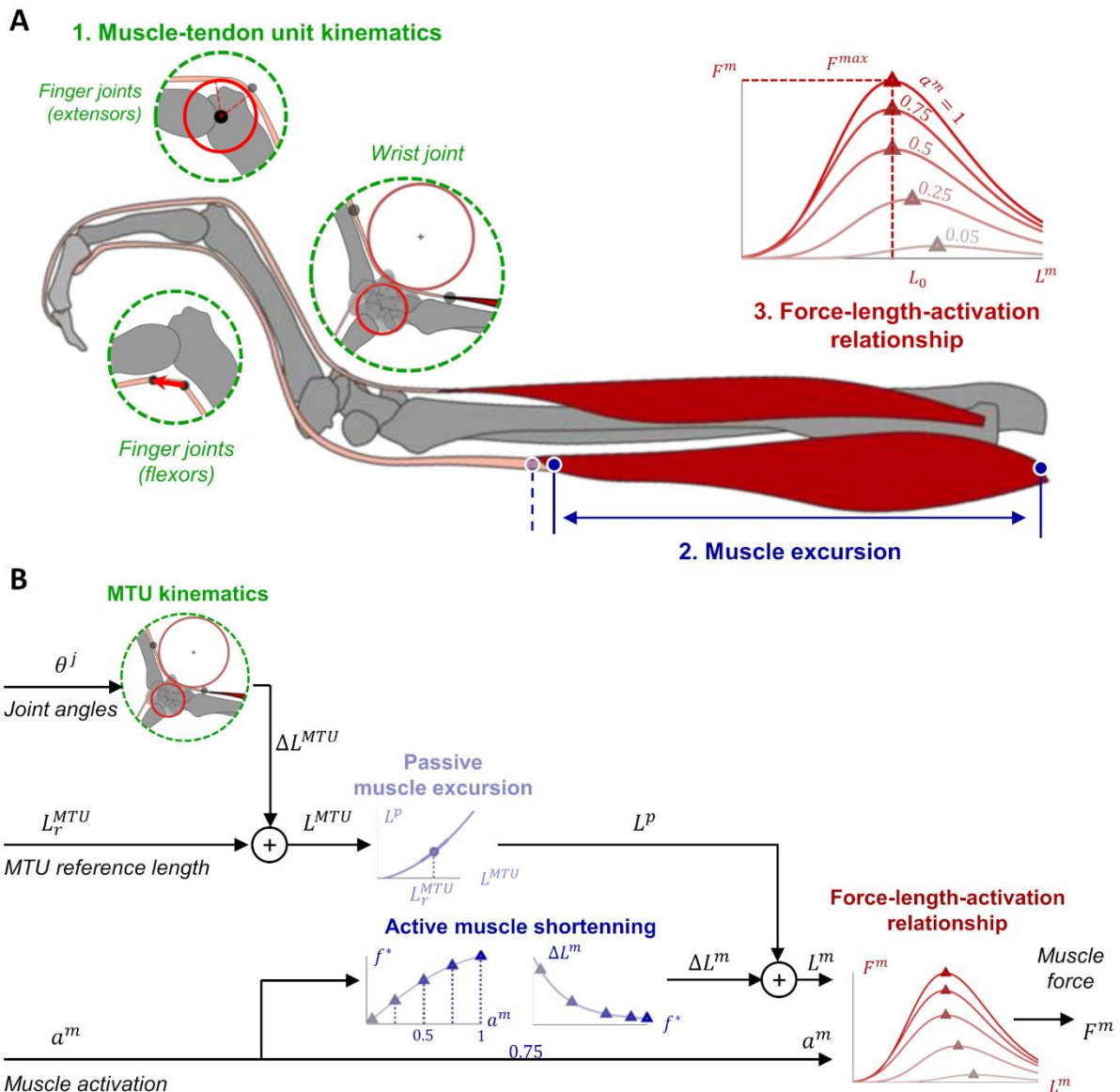


Figure s2.1 – Illustrations describing the musculoskeletal model principle. All symbols and variables are described in the text.

The MTU excursion model at the index finger joints (DIPi, PIPi, MCPi) relied on the normative tendon path data and the geometrical models provided by Chao et al.<sup>3</sup> (Chapter 1). Tendon path data is normalized by middle phalanx length and was thus scaled back to each subject via regression equation provided by Buchholz *et al.*<sup>1</sup> using the measured hand length. For finger extensors (EDC), the tendon is considered to wrap on a cylinder which axis is aligned with the joint flexion-extension axis such that the excursion  $\Delta L_j^{mtu}$  was the product of the tendon moment arm and the joint angle, i.e., Landsmeer Model I<sup>9</sup> (Figure s2.1A). The effect of extensor mechanism on MTU excursion was neglected and the excursion of EDC at DIPi and

PIPi were those of the terminal extensor (TE) and extensor slip (ES), respectively. For finger flexors (FDS), the tendon is represented by two points, one proximal and one distal to the joints, and the excursion  $\Delta L_j^{mtu}$  is determined as the variation of the distance between the two points, i.e., bow-string model<sup>3</sup> (Figure s2.1A).

The MTU excursion at the wrist joint was determined using a custom model<sup>2</sup> relying on anatomical data and the double-cylinder geometrical model developed by Goislard de Monsabert *et al.*<sup>5</sup> (Figure s2.1A). The tendon was considered to wrap alternatively on two cylinders, representing either bony (carpals) or ligamentous (retinacula) structures. The tendon is described by two points, one proximal and one distal to the wrist joint and its path was determined by the shortest path method<sup>4</sup> using either one of the cylinder as obstacle if the tendon is crossing one of them or none if the tendon is between them. The two points describing tendon path at the wrist were taken from the anatomical dataset of Goislard de Monsabert *et al.*<sup>5</sup>. Parameters of the two cylinders were the same as in the previous study on power grip, i.e., determined via an optimisation procedure<sup>2</sup>, and are given in Table s2.1.

### Muscle belly excursion

The current muscle belly length ( $L^m$ ) was determined removing the active muscle belly shortening ( $\Delta L^m$ ) from the passive belly length ( $L^p$ ), i.e., before contraction.

$$L^m = L^p - \Delta L^m \quad \text{Equation 2}$$

The passive belly length varies with the tendon lengthening/shortening when joint posture changes and was described here as a function of the current MTU length:

$$L^p(L^{mtu}) = p_2(L^{mtu})^2 + p_1L^{mtu} + p_0 \quad \text{Equation 3}$$

Where  $\mathbf{d} = \{d_2; d_1; d_0\}$  are polynomial coefficients that were determined in previous studies<sup>6,7</sup> from ultrasound imaging and motion capture experimental data. The values of those coefficients are provided in Table s2.2

The active muscle belly shortening ( $\Delta L^m$ ), corresponding to muscle length decrease with active contraction of the fibres was determined from activation ( $a^m$ ) with two relationships. The first relationship estimates a virtual muscle force level ( $f^*$ ) using a sigmoid function (Equation 4; Figure s2.1B).

$$F^*(a^m) = \alpha_1 \left[ \frac{1}{1 + \exp(-\alpha_2 (a^m - \alpha_3))} - 0.5 \right] + \alpha_4 \quad \text{Equation 4}$$

Where  $\alpha = \{\alpha_3; \alpha_2; \alpha_1\}$  are coefficients describing the sigmoid function that were determined in previous studies from electromyography and dynamometry experimental data<sup>6,7</sup>. The values of those coefficients are provided in Table s2.3. The second relationship estimates the muscle

active shortening  $\Delta L^m$  during contraction from the virtual force level and is described by an exponential function (Equation 5 Figure s2.1B).

$$\Delta L^m(F^*) = \gamma_1 [1 - \exp(-\gamma_2 F^*)] \quad \text{Equation 5}$$

Where  $\boldsymbol{\gamma} = \{\gamma_2; \gamma_1\}$  are coefficients describing the exponential function and were determined in previous studies from dynamometry, ultrasound and motion capture experimental data<sup>6,7</sup>. The values of those coefficients are provided in Table s2.4.

### Force-length-activation relationship

The muscle force was estimated from muscle belly length ( $L^m$ ) and muscle activation ( $a^m$ ) using a force-length-activation relationship (Figure s2.1B). This relationship relied on the equations of Kaufman et al.<sup>8</sup> (Equations 7a-d) describing force-length behaviour at maximal activation ( $a^m = 1$ ) and was adapted to include activation-dependency of the muscle contraction. This adaptation was done by considering the effect of activation on the three main parameters describing muscle isometric strength, i.e., index of architecture ( $i_a$ ), optimal belly length ( $L_0$ ) and maximal isometric force ( $F_0$ ) (Equations 6a-c). The first step was thus to compute these parameters using the following polynomial relationship

$$i_a = b_5(a^m)^5 + b_4(a^m)^4 + b_3(a^m)^3 + b_2(a^m)^2 + b_1 a^m + b_0 \quad \text{Equation 6a}$$

$$L_0 = c_5(a^m)^5 + c_4(a^m)^4 + c_3(a^m)^3 + c_2(a^m)^2 + c_1 a^m + b_0 \quad \text{Equation 6b}$$

$$F_0 = d_3(a^m)^3 + d_2(a^m)^2 + d_1 a^m \quad \text{Equation 6c}$$

Where  $\mathbf{b} = \{b_5; b_4; b_3; b_2; b_1; b_0\}$ ,  $\mathbf{c} = \{c_3; c_2; c_1; c_0\}$  and  $\mathbf{d} = \{d_3; d_2; d_1; d_0\}$  are polynomial coefficients that were determined in previous studies<sup>6,7</sup>. The values of those coefficients are provided in Table s2.5, s2.6 and s2.7. The second step consisted in estimating muscle force from muscle belly length using the calculated parameters in the equation of Kaufman *et al.*

$$F^m(L^m) = F_0 \cdot \exp \left[ - \left( \frac{(\varepsilon^m + 1)^\beta - 1}{\omega} \right)^\rho \right] \quad \text{Equation 7a}$$

with

$$\varepsilon^m = \frac{L^m - L_0}{L_0} \quad \text{Equation 7b}$$

$$\omega = 0.35327(1 - i_a) \quad \text{Equation 7c}$$

$$\beta = 0.96343 \left( 1 - \frac{1}{i_a} \right) \quad \text{Equation 7d}$$

Where  $\varepsilon^m$  was the muscle strain and  $\omega$ ,  $\beta$  and  $\rho$  were shape parameters of the force-length relationship corresponding to width, skewness and roundness, respectively. Roundness  $\rho$  was equal to  $2^{6,7}$ .

### Associated data

Table s2.1 – Antero-posterior ( $X_{c1}$ ) and longitudinal ( $Y_{c1}$ ) coordinates (in mm) and radius (in mm) of the cylinders used for determining tendon path and muscle-tendon unit excursion as a function of wrist angular position. The tendon path of each muscle is determined by two cylinders (C1 and C2).

	$X_{c1}$	$Y_{c1}$	$R_{c1}$	$X_{c2}$	$Y_{c2}$	$R_{c2}$
FCR	3	-5.6	15	25	1.17	5.1
FDS	2.38	2.39	12.34	22.58	11.26	2.66
ECR	-13.08	25.77	15	-5.88	1.57	6
EDC	-9.98	14.27	3	3.59	1.02	13.39

Table s2.2 – Coefficients of the polynomial regression between normalized passive belly length ( $l^p$ ) and normalized muscle-tendon unit length ( $l^{mtu}$ ). To use as follows  $l_1^m = p_2(l^{mtu})^2 + p_1 l^{mtu} + p_0$ . Muscle-tendon unit length is normalized by dividing by the reference muscle-tendon unit length ( $L_r^{MTU}$ ). Passive muscle belly length is normalized by dividing it by its value at reference posture, i.e., using  $L^{MTU} = L_r^{MTU}$  in equation 2.

	$p_2$	$p_1$	$p_0$
FCR	-0.66	2.70	-1.05
FDS	12.63	-23.78	12.15
ECR	25.97	-48.21	23.25
EDC	15.71	-29.60	14.90

Table s2.3 – Coefficients of the relationship between normalized virtual force ( $f^*$ ) and muscle activation ( $a^m$ ). To use as follows:  $f^*(a^m) = \alpha_1 \left[ \frac{1}{1 + \exp^{-\alpha_2(a^m - \alpha_3)}} - 0.5 \right] + \alpha_4$ . Virtual force is normalized by dividing by  $F^{max}$ , i.e., the maximal isometric force  $F^0$  at maximal activation ( $a^m = 1$ ). Muscle activation  $a^m$  is unitless and equal to 1 during a maximal voluntary contraction.

	$\alpha_1$	$\alpha_2$	$\alpha_3$	$\alpha_4$
FCR	0	0	2.07	2.95
FDS	0	0	1.92	5.15
ECR	0.096	0.13	2.01	2.72
EDC	0.33	0.40	1.27	4.47

Table s2.4 – Coefficients of the relationship between normalized muscle active shortening ( $\Delta l^m$ ) and normalized virtual force  $f^*$ . To use as follows:  $\Delta l^m(f^*) = \gamma_1 [1 - \exp(-\gamma_2 f^*)]$ . Virtual force is normalized by dividing by  $F^{max}$ , i.e., the maximal isometric force  $F^0$  at maximal activation ( $a^m = 1$ ). Muscle active shortening was normalized by dividing by passive muscle belly length at reference posture, i.e., using  $L^{MTU} = L_r^{MTU}$  in equation 2. A positive  $\Delta l^m$  corresponds to muscle shortening.

	$\gamma_1$	$\gamma_2$
FCR	0.043	4.37
FDS	0.046	3.09
ECR	0.069	3.61
EDC	0.028	3.72

Table s2.5 – Coefficients of the polynomial regression between the index of architecture ( $i_a$ ) and the activation level ( $a^m$ ). The coefficients are used as follows:  $i_a = b_5(a^m)^5 + b_4(a^m)^4 + b_3(a^m)^3 + b_2(a^m)^2 + b_1 a^m + b_0$ . Muscle activation  $a^m$  is unitless and equal to 1 during a maximal voluntary contraction. Index of architecture  $i_a$  is unitless.

	$b_5$	$b_4$	$b_3$	$b_2$	$b_1$	$b_0$
FCR	0.714	-2.399	2.463	-0.701	0.069	0.169
FDS	-2.560	6.488	-5.206	1.098	0.192	0.188
ECR	-0.664	2.575	-3.404	1.712	-0.157	0.231
EDC	-0.105	0.308	-0.697	0.792	-0.167	0.173

Table s2.6 – Coefficients of the polynomial regression between normalized optimal length ( $l_0$ ) and muscle activation ( $a^m$ ). To use as follows:  $l_0 = c_5(a^m)^5 + c_4(a^m)^4 + c_3(a^m)^3 + c_2(a^m)^2 + c_1 a^m + c_0$ . Optimal length  $L_0$  was normalized by dividing by the passive muscle belly length at reference posture, i.e., using  $L^{MTU} = L_r^{MTU}$  in equation 2. Muscle activation  $a^m$  is unitless and equal to 1 during a maximal voluntary contraction. Index of architecture  $i_a$  is unitless.

	$c_5$	$c_4$	$c_3$	$c_2$	$c_1$	$c_0$
FCR	0.096	-0.335	0.330	-0.042	-0.099	1.002
FDS	-0.417	1.551	-2.197	1.461	-0.445	0.997
ECR	0	0	-0.048	0.196	-0.211	0.971
EDC	0	0	-0.050	0.107	-0.083	1.016

Table s2.7 – Coefficients of the polynomial regression between the normalised maximal force ( $f_0$ ) and the activation level ( $a^m$ ). The coefficients are used as follows:  $f_0 = d_3(a^m)^3 + d_2(a^m)^2 + d_1a^m$ . Maximal force was normalized by dividing by  $F^{max}$ , i.e., the maximal isometric force  $F^0$  at maximal activation ( $a^m = 1$ )

	$d_3$	$d_2$	$d_1$
FCR	0.297	-1.430	2.120
FDS	0.766	-2.522	2.754
ECR	-0.029	-0.336	1.361
EDC	-0.528	0.025	1.484

## References

1. Buchholz, B., T. J. Armstrong, and S. A. Goldstein. Anthropometric data for describing the kinematics of the human hand. *Ergonomics* 35:261–273, 1992.
2. Caumes, M., B. Goislard de Monsabert, H. Hauraix, E. Berton, and L. Vigouroux. Complex couplings between joints, muscles and performance: the role of the wrist in grasping. *Sci. Rep.* 9:1–11, 2019.
3. Chao, E. Y., K. N. An, W. P. Cooney III, and R. L. Linscheid. Biomechanics of the hand: a basic research study. Singapore: World Scientific, 1989, 208 pp.
4. Charlton, I. W., and G. R. Johnson. Application of spherical and cylindrical wrapping algorithms in a musculoskeletal model of the upper limb. *J. Biomech.* 34:1209–1216, 2001.
5. Goislard De Monsabert, B., D. Edwards, D. Shah, and A. Kedgley. Importance of Consistent Datasets in Musculoskeletal Modelling: A Study of the Hand and Wrist. *Ann. Biomed. Eng.* 46:71, 2018.
6. Goislard de Monsabert, B., H. Hauraix, M. Caumes, A. Herbaut, E. Berton, and L. Vigouroux. Modelling force-length-activation relationships of wrist and finger extensor muscles. *Med. Biol. Eng. Comput.* 58:2531–2549, 2020.
7. Hauraix, H., B. Goislard De Monsabert, A. Herbaut, E. Berton, and L. Vigouroux. Force–Length Relationship Modeling of Wrist and Finger Flexor Muscles. *Med. Sci. Sports Exerc.* 50:2311–2321, 2018.
8. Kaufman, K. R., K. N. An, and E. Y. Chao. Incorporation of muscle architecture into the muscle length-tension relationship. *J. Biomech.* 22:943–948, 1989.
9. Landsmeer, J. M. Studies in the anatomy of articulation. I. The equilibrium of the “intercalated” bone. *Acta Morphol. Neerl. Scand.* 3:287–303, 1961.